Journal of Marine Science and Technology

Volume 23 | Issue 6 Article 8

STATISTICAL ANALYSIS ON THE LONG-TERM OBSERVATIONS OF TYPHOON WAVES IN THE TAIWAN SEA

Dong-Jiing Doong
Department of Hydraulic and Ocean Engineering, National Cheng Kung University, Tainan, Taiwan, R.O.C.

Cheng-Han Tsai
Department of Marine Environmental Informatics, National Taiwan Ocean University, Keelung, Taiwan, R.O.C., chtsai@mail.ntou.edu.tw

Ying-Chih Chen
Department of Marine Environmental Informatics, National Taiwan Ocean University, Keelung, Taiwan, R.O.C.

Jen-Ping Peng
Department of Marine Environmental Informatics, National Taiwan Ocean University, Keelung, Taiwan, R.O.C.

Ching-Jer Huang
Department of Hydraulic and Ocean Engineering, National Cheng Kung University, Tainan, Taiwan, R.O.C. Coastal Ocean Monitoring Center, National Cheng Kung University, Tainan, Taiwan, R.O.C.

Recommended Citation

Doong, Dong-Jiing; Tsai, Cheng-Han; Chen, Ying-Chih; Peng, Jen-Ping; and Huang, Ching-Jer (2015) "STATISTICAL ANALYSIS ON THE LONG-TERM OBSERVATIONS OF TYPHOON WAVES IN THE TAIWAN SEA," *Journal of Marine Science and Technology*: Vol. 23: Iss. 6, Article 8.
DOI: 10.6119/JMST-015-0610-7
Available at: https://jmstt.ntou.edu.tw/journal/vol23/iss6/8

STATISTICAL ANALYSIS ON THE LONG-TERM OBSERVATIONS OF TYPHOON WAVES IN THE TAIWAN SEA

Acknowledgements

The authors would like to thank the Central Weather Bureau (MOTC-CWB-104-O-03) and the Ministry of Science and Technology (MOST 101-2628-E-006-024-MY3) for their support of this study.

Journal of Marine Science and Technology, Vol. 23, No. 6, pp. 893-900 (2015)
DOI: 10.6119/JMST-015-0610-7

STATISTICAL ANALYSIS ON THE LONG-TERM OBSERVATIONS OF TYPHOON WAVES IN THE TAIWAN SEA

Dong-Jiing Doong[1], Cheng-Han Tsai[2], Ying-Chih Chen[2], Jen-Ping Peng[2], and Ching-Jer Huang[1, 3]

Key words: typhoon wave, data buoy, equilibrium range slope, JONSWAP spectrum.

ABSTRACT

Seventeen data buoys were deployed in the Taiwan Sea since 1997. These buoys have made measurement for more than 100 typhoons. The purpose of this paper is to study the statistical characteristics of the observed typhoon waves. High resolution directional wave spectra are obtained by analyzing the buoy data. The Significant Typhoon Wave Height (SWTH) and the Duration of Large Waves (DLW) are proposed to indicate the sea severity of typhoons. The joint effect of the SWTH and the DLW is used to assess possible impact by the typhoon waves to the coast, using the damage curve calibrated from historical events. In addition analysis on the slope of the equilibrium range on the high-frequency side of the typhoon wave frequency spectra shows that its slope is less than 3.5 in absolute value for coastal water and larger than 3.8 for the deep sea. The JONSWAP spectrum model is then used to fit the mean wave spectra of the largest sea state in typhoons. It is found that the peak-enhancement factors γ obtained were 2.48 and 2.19 for the deep sea and the coastal ocean, respectively, showing that typhoon waves in Taiwan sea are in the developing stage.

I. INTRODUCTION

The Northwestern Pacific Ocean is an area encounters the most frequent typhoons in the world. Not only strong wind, typhoons also bring heavy rain, large storm surge and huge waves, which may cause damages to coastal defense structures, resulting in floods and loss of human lives and properties. Starting from 1997, when Taiwan deployed its first operational data buoy to the end of 2014, the Central Weather Bureau (CWB) has issued warnings for 105 typhoons. Fig. 1 shows the tracks of these typhoons. On average, 5.8 typhoon warnings were issued each year, which is 66% higher than the long-term (1895-1995) historical average of 3.5. Among the 105, fifty-four (51%) typhoons either reached within 100 km from the coast of Taiwan or landed on Taiwan. Hence, the coasts of Taiwan are prone to be ravaged by typhoons.

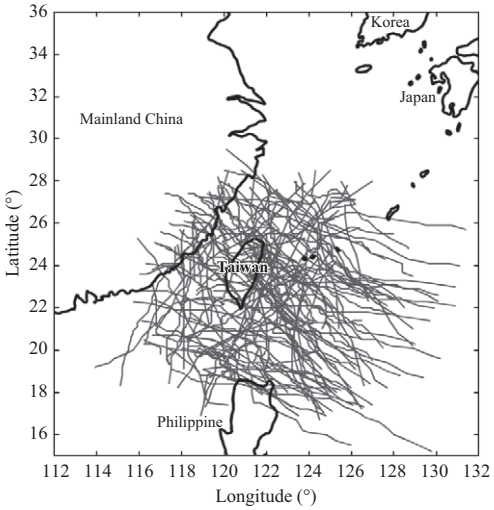

Fig. 1. Tracks of typhoons approaching Taiwan between 1997 and 2014.

Field measurements of sea state, particularly during the passage of typhoons, are essential for the design of coastal protection and planning of marine activities. They are also needed for numerical model calibration and verification. Moreover, since typhoons generate severe sea states, typhoon wave data are required for calculating peak loads on coastal structures. Since 1972, the National Oceanic and Atmospheric Administration (NOAA) in the US, has deployed buoys at various locations around US coast to measure ocean waves.

Paper submitted 11/25/14; revised 02/01/15; accepted 06/10/15. Author for correspondence: Cheng-Han Tsai (e-mail: chtsai@mail.ntou.edu.tw).
[1]Department of Hydraulic and Ocean Engineering, National Cheng Kung University, Tainan, Taiwan, R.O.C.
[2]Department of Marine Environmental Informatics, National Taiwan Ocean University, Keelung, Taiwan, R.O.C.
[3]Coastal Ocean Monitoring Center, National Cheng Kung University, Tainan, Taiwan, R.O.C.

Fig. 2. Photo of the data buoy deployed in Taiwan sea.

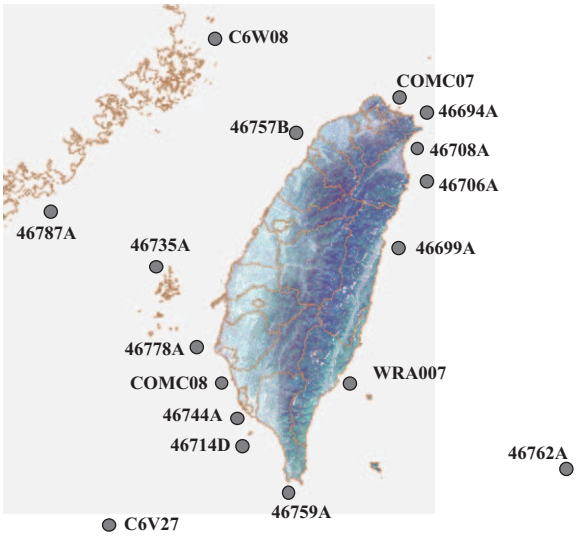

Fig. 3. Locations of the data buoys in Taiwan sea.

The Ocean Data Gathering Program (Shemdin, 1977; Ward, 1974) was the first comprehensive attempt to collect hurricane data in the Gulf of Mexico. In Australia, a large hurricane wave database was established in 1970 and many results were presented, especially on the typhoon spectra (Young, 1998; 2003). In Taiwan, a long-term, operational coastal ocean monitoring network, which includes data buoys, tidal stations, coastal weather stations, coastal cameras and radars, was developed and implemented in 1997 in the Taiwan sea. The network has since collected sizable data sets, which included typhoon wave information.

In recent years, there has been major interest in the issues concerning global change, which includes the changes in wave climate. These changes must be understood to enable coastal managers and researchers to determine how the changes, if any, will have impacts on the coastal infrastructure and environment. In this study, in-situ data measured by buoys during typhoons from 1997 to 2014 (18 years) in the Taiwan sea are investigated.

II. BUOY NETWORK IN TAIWAN SEA

As previously mentioned, a marine monitoring network has been established in the Taiwan sea since 1997. The network is comprised of 17 data buoys and numerous tidal and coastal weather stations. The wave data were measured by 2.5 m-diameter discus type buoys (Fig. 2). The buoys are powered by solar panels, which charge on-board batteries to ensure uninterrupted operation at night and in bad weather. To obtain real-time data, the buoys are equipped with at least two of the following data transmission devices: radio telemetry, GSM, GPRS or iridium satellite communications, depending on the buoy location.

The buoys were developed by the Coastal Ocean Monitoring Center (COMC) of the National Cheng Kung University (NCKU) and to measure ocean waves and other meteorological data such as wind speed, wind direction, wind gusts, barometric pressure, air temperature and surface water temperature. The buoys are equipped with heave, pitch, and roll accelerometers, sampling at 2 Hz frequency for 10 minutes in each hour. A rigorous data quality checking system was applied to the buoy system to ensure the quality of the measurements (Doong et al., 2007). Fig. 3 shows the location of the buoys. Location, station depth and year of first deployment of the buoys are listed in Table 1. Fig. 4 shows the successful observation rates for the buoys; they range from 84% to 99% with a 92% average success rate. The line in Fig. 4 indicates the number of typhoon datasets collected by the respective buoy.

III. ANALYSIS OF TYPHOON WAVE RECORDS

To conserve power and to reduce processing time as well as the cost for data transmission, the frequency resolution of the directional wave spectra analyzed onsite at the buoys is set 0.0085 Hz, i.e. 41 frequency bands for 0.05 to 0.4 Hz. The spectral resolution is not sufficient for research purposes, however. Raw data from the buoys were re-analyzed in this study to obtain high resolution wave spectra with 128 frequency bands and the corresponding wave parameters.

The directional wave spectrum $S(f,\theta)$ is the fundamental property of ocean waves, which expresses the energy distribution as a function of the wave frequency $S(f)$ and the direction of wave propagation $G(\theta|f)$. The directional wave spectrum is expressed as:

$$S(f,\theta) = S(f)G(\theta|f) \tag{1}$$

Longuet-Higgins et al. (1963) approximates the directional distribution by a Fourier series expansion,

Table 1. List of the long-term operational data buoys in Taiwan sea.

Buoy code	Location (abbr.)	Depth*	Record duration	Qty. of typhoon data collected
46694A	Longdong (LD)	23 m	1998 -	95
46708A	Gueisandao (GSD)	28 m	2002 -	76
46706A	Suao (SA)	20 m	1999 -	92
46699A	Hualien (HL)	30 m	1997 -	101
46759A	Eluanbi (ELB)	40 m	2000 -	84
46714D	Xiaoliuqiu (XLC)	82 m	2003 -	60
46744A	Dapeng Bay (DPB)	26 m	2002 -	62
46778A	Qigu (QG)	18 m	2006 -	41
46735A	Penghu (PH)	20 m	2006 -	42
46787A	Kinmen (KM)	25 m	2000 -	86
46757B	Hsinchu (HC)	17 m	1997 -	96
C6S62	Taitung Deep Sea (TDS)	5000 m	2006 -	21
C6V27	Dongsha (DS)	2600 m	2010 -	26
C6W08	Matsu (MT)	58 m	2010 -	25
WRA007	Taitung (TT)	30 m	2010 -	21
COMC08	Mituo (MO)	23 m	2012 -	12
COMC07	Keelung (KL)	40 m	2012 -	8

*may change due to re-deployment.

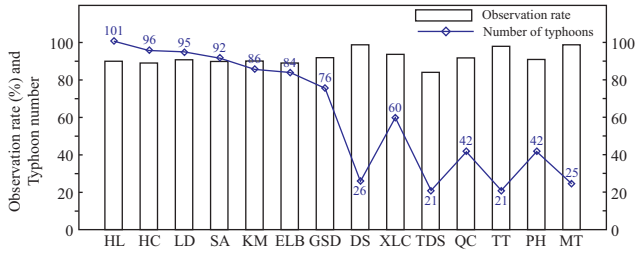

Fig. 4. Successful observation rate and quantity of typhoon data collected by each buoys.

$$\left(\theta\middle|f\right)=\frac{1}{2}+\sum_{n=1}^{\infty}\left[a_n\left(f\right)\cos n\theta+b_n\left(f\right)\sin n\theta\right] \qquad (2)$$

where a_n and b_n are the Fourier coefficients of the n^{th} harmonic component. The Fourier coefficients of the first two harmonic terms can be computed from the co and quad-spectra of buoy's heave and the north–south and east–west slopes. A cross spectrum is defined as the Fourier transform of the cross correlation function of two time series:

$$R_{ij}(\tau)=\lim_{T\to\infty}\frac{1}{T}\int_{-T/2}^{T/2}\eta_i(t)\eta_j(t+\tau)dt \qquad (3)$$

$$\Phi_{ij}\left(f\right)=\int_{-\infty}^{\infty}R_{ij}\left(\tau\right)e^{-2\pi i f\tau}d\tau \qquad (4)$$

where $\Phi_{ij}(f)$ is the cross spectrum; $R_{i,j}(\tau)$ is the cross correlation function at the sites, i and j; η_i, η_j are the surface elevation at i and j; τ is the time lag; and T is the sampling time.

Isobe (1984) presented the general form of the relationship between the cross spectrum and the directional spectrum, as shown in Eq. (5):

$$\Phi_{ij}\left(f\right)=\int_0^{2\pi}H_i\left(f,\theta\right)\cdot\overline{H_{jn}}\left(f,\theta\right)\cdot \left\{\begin{matrix}\cos\left[k\cdot\left(x_{ij}\cos\theta+y_{ij}\sin\theta\right)\right]\\ -i\sin\left[k\left(x_{ij}\cos\theta+y_{ij}\sin\theta\right)\right]\end{matrix}\right\} \cdot S\left(f,\theta\right)d\theta \qquad (5)$$

where $\Phi_{ij}(f)$ is the cross spectrum, $H_i(f,\theta)$ is the transformation function, and $\bar{H}_j(f,\theta)$ is the conjugate function of $H_i(f,\theta)$. The directional wave spectrum is derived by solving Eqs. (1), (2) and (5). Fig. 5 shows an example of the frequency spectrum obtained after re-analysis.

The comprehensive comparison study was carried out in this research. Fig. 6 shows the comparisons of H_{m0} and T_{m02} between the re-analysis and the operational derivations in the TDS buoy, as an example. The definition of H_{m0} and T_{m02} are $H_{m0}=4.004\sqrt{m_0}$ and $T_{m02}=\sqrt{m_0/m_2}$ respectively, where m_n is n^{th} moment of a wave spectrum. Quantitative results show that the bias of significant wave height between the operational and re-analysis is 3.52%, bias for the mean wave period is 2.26%, and more than 70% of the peak period biases are less than 0.01 Hz. More than 70% of the dominant direction biases are less than 10 degrees. Re-analysis of the raw buoy data obtains statistical wave parameters that are

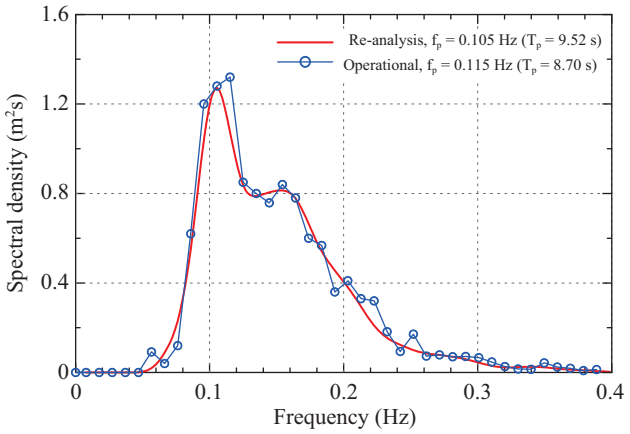

Fig. 5. Comparison of the frequency spectra obtained from the operational buoy and after re-analysis.

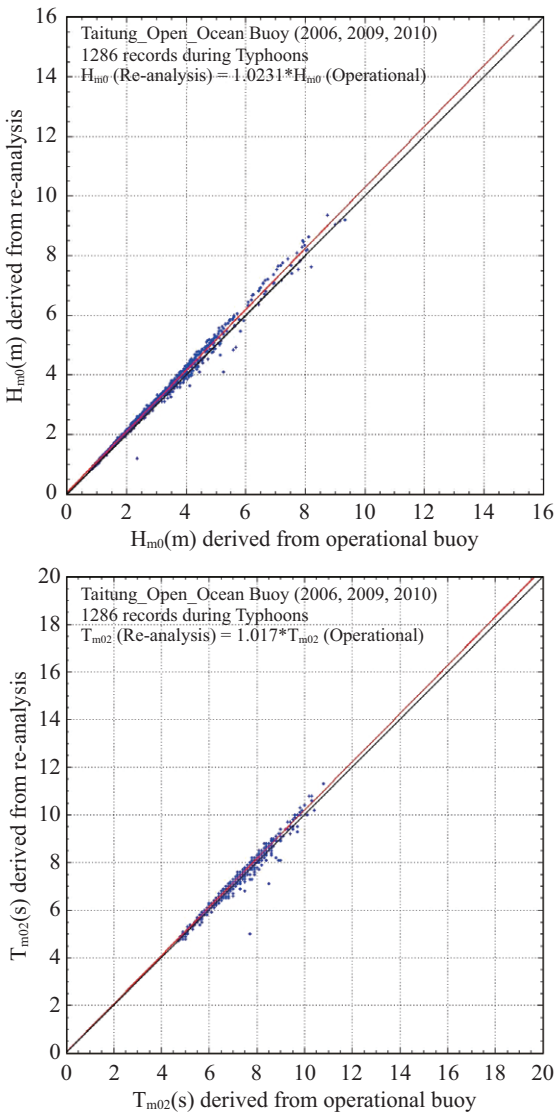

Fig. 6. Comparison of the SWH (H_{m0}) and the mean wave period (T_{m02}) between the re-analysis and the operational derivations in the TDS buoy.

Table 2. Extreme waves observed during typhoons (SWH: significant wave height, STWH: significant typhoon wave height, DLW: duration of large waves, STWH and DLW are calculated from all typhoons, not just the one indicated in the table, each buoy recorded).

Buoy	Observed max. SWH (m)	In the typhoon (year)	STWH Mean ± Std (m)	DLW Mean ± Std (hr)
LD	11.15	Jangmi (2008)	3.4 ± 1.8	4.5 ± 3.4
GSD	23.94	Krosa (2007)	3.3 ± 1.8	3.7 ± 3.5
SA	15.05	Fanap (2010)	3.5 ± 2.3	3.1 ± 2.6
HL	11.94	Amber (1997)	3.0 ± 1.8	4.2 ± 2.9
ELB	14.13	Usagi (2013)	3.3 ± 1.9	5.4 ± 7.7
XLC	12.74	Morakot (2009)	3.1 ± 1.8	3.8 ± 3.0
QG	11.71	Linfa (2009)	3.4 ± 2.0	4.4 ± 2.9
DPB	8.99	Morakot (2009)	3.0 ± 1.5	3.4 ± 1.6
PH	6.07	Megi (2010)	2.5 ± 0.8	5.5 ± 4.1
KM	9.12	Fanap (2010)	2.5 ± 1.2	3.0 ± 1.9
HC	12.45	Jangmi (2008)	2.1 ± 1.3	4.2 ± 3.9
TDS	18.88	Jelawat (2012)	5.6 ± 3.1	6.2 ± 6.7
DS	13.42	Usagi (2013)	3.4 ± 1.8	5.4 ± 3.4
MT	12.45	Tembin (2013)	4.3 ± 3.1	3.1 ± 0.9
TT	12.13	Usagi (2013)	3.3 ± 2.2	4.2 ± 3.4
KL	7.94	Fitow (2013)	4.2 ± 2.3	5.9 ± 5.5

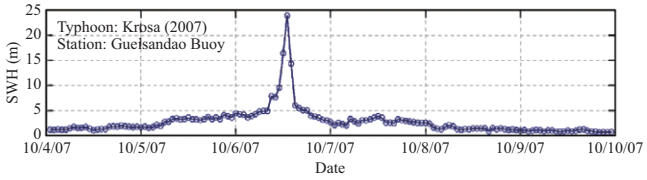

Fig. 7. Time series of the SWH observed at the Longdong Buoy during typhoon Krosa (2007).

consistent with that onsite operationally derived. However, the resolution of the re-analyzed wave spectra is improved.

IV. SEVERITY OF A TYPHOON

1. Extreme Waves

Extreme wave height is typically used to represent sea state conditions during a typhoon. Many studies have presented the existence of gigantic waves during a hurricane or typhoon in the world oceans (Wang, et al., 2005; Holliday et al., 2006). The maximum significant wave heights observed by the Taiwanese buoys are listed in Table 2. For example, a record of significant wave height of 23.94 m was observed by GSD during the Typhoon Krosa in 2007 (Fig. 7). This record has been verified by examining the raw data (Liu et al., 2008), and numerical simulation was carried out to understand the cause of such a severe event (Babanin et al., 2011).

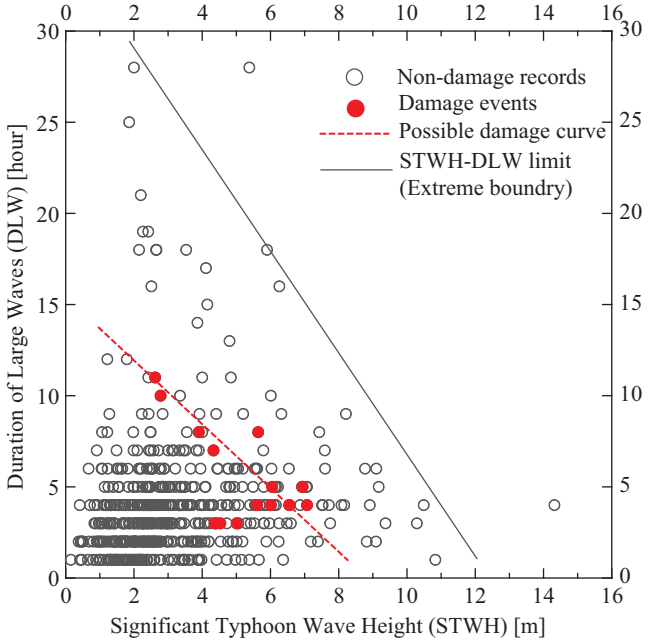

Fig. 8. Scatter plot of the STWH and DLW. Open circles are the data from all buoys observed during typhoons. Solid circles represent events with costal damages.

2. Significant Typhoon Wave Parameters

Typhoons are complex events that cannot be presented with only a maximum wave height record. Extreme typhoon waves cause huge impact on the coast but with a short duration. For example, the CWB's warning for the 2007 Typhoon Krosa was issued for 78 hours, but the sea-state of 23.94 m lasted only 1 hour. Hence, the extreme wave may not be the best parameter to indicate the severity of a typhoon sea state. This study proposes two parameters to better represent typhoon severity: the Significant Typhoon Wave Heights (STWH) and the Duration of Large Waves (DLW). Following the definition of significant wave height, the STWH (unit: m or cm) is defined as the mean value of the highest one third of the waves during the time under the action of typhoon. The DLW is the time length (unit: hour) of the wave height in a typhoon when it is larger than the STWH. The time length under the action of typhoon is defined as the time period when the distance of a typhoon center is 300 km to the station. The average STWHs and corresponding DLWs for all collected typhoon data for each buoy are listed in Table 2. The standard deviations for both parameters are large, indicating that the typhoon waves varied significantly from typhoon to typhoon. From the table, it can be seen that the mean STWHs are much less than the observed maximum significant wave heights; however, their impact on the coast cannot be neglected when considering the action time (DLW) of the STWH.

STWH and DLW can be used to assess potential damages to coastal infrastructures such as sea dykes, harbor breakwaters and coastal highways. Fig. 8 plots the STWH versus the DLW. Each data pint represents the STWH and its corresponding

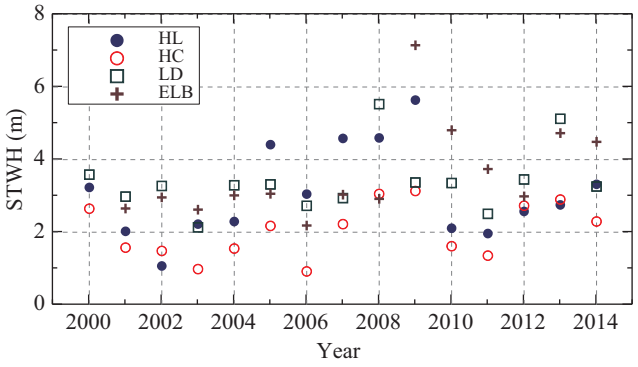

Fig. 9. Yearly variation of the significant typhoon wave height (STWH) observed at the four buoy stations

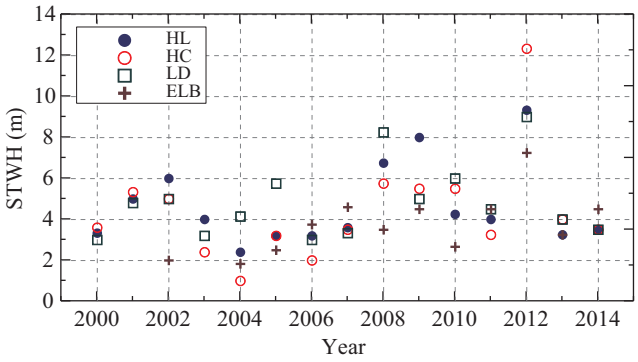

Fig. 10. Yearly variation of the duration of large wave (DLW) observed at the four buoy stations.

DLW in a typhoon. The plot collects the data from all buoys. The upper limit of all data points is also delineated in the figure. The solid circles in the figure are the events with known coastal damage according to damage reports, and the possible damage curve is therefore given in the figure. When the plotting position of STWH and the DLW of a typhoon is on the right-hand side of this curve, coastal damage may occur. Well-protected coastlines may account for some sea states that were more severe than the limit curve to sustain no damages.

3. Long-Term Trend

Figs. 9 and 10 show the yearly variations of the STWH and the DLW since 2000, respectively. The data are from four buoys located in the northern (Longdong), eastern (Hualien), southern (Eluanbi), and western (Hsinchu) parts of the Taiwan sea. It is to note that only the mean values of each parameter are shown in the figure. From the figures, it is clear that the STWH ranged from 2 to 4 m, and the DLW lasted between 2 to 6 hours. This numbers do not appear to be large; however, they are actually quite severe when coupled with the wind and storm surge.

Global climate change may have impacts on sea states. The trend of increasing wave height in the Northeast Atlantic was identified in the late 1980s and early 1990s (Carter and Draper,

1988; Bacon and Carter, 1991). It was suggested the mean wave height has increased 2% per year. More recent studies have identified similar changes in the Pacific (Allan and Komar, 2000). Several related studies were presented (Weisse et al., 2005; Wang and Swail, 2006; Weisse and Günther, 2007; Grabemann and Weisse, 2008). The two parameters proposed in this study can be used to examine the trend of typhoon waves. In Figs. 9 and 10, it is found that the STWH and the DLW have significant increasing trends between 2000 and 2009. This means that the typhoon generated waves became severe in the early 21st century; however, there is a downward trend from 2009 to 2010. Then, between 2010 and 2014, another increasing trend appeared. Apparently, much more data are required to see whether the trend has a decadal variability.

V. TYPHOON WAVE SPECTRA

1. Spectral Slope

The typhoon-generated waves that have large spatial and temporal variations are significantly different from those observed during non-typhoon period. This is due to the rapid change of wind intensity and direction. The rate of change of wind speed in the path of a typhoon is much greater than that in other weather conditions. The duration of a given wind speed during a typhoon is also extremely short in contrast to the winds in other conditions when the wind blows continuously for several hours with constant speed. These characteristics are addressed by the shape of the typhoon wave spectra.

The slope of the equilibrium range on the high-frequency side of a wind wave frequency spectrum has been discussed over the last 50 years. The smaller-scale waves that control these parts of the spectra are important because they largely determine the momentum exchange between the atmosphere and the ocean (Makin et al., 1995). Recently, this equilibrium range has gained more significance following developments in remote sensing. Phillips (1958) inferred that a range of frequencies on the high-frequency side of the spectrum will be dynamically saturated between the energy input and dissipation processes, independent of wind stress, and proportional to the -5 power of frequency based on dimensional considerations. Since then, oceanographers and coastal engineers have adhered to this -5th equilibrium range concept. However, The f^{-4} spectral shape was first suggested as a universal form, based on observations by Toba (1973). Phillips (1985) re-examined the processes of energy input from wind stress, wave breaking, and wave-wave interactions and revised his earlier concept by theoretically concluding that the frequency spectrum $S(f)$ is in fact proportional to $gu_* f^{-4}$, where u_* is the wind friction velocity. The ocean wave community has accepted this concept since then; however, what is the slope of the equilibrium range in the frequency spectrum of typhoon waves? In this paper this question is explored, using a large number of measured typhoon wave spectra in Taiwan sea to make a detailed examination of the equilibrium range slope of a wave spectrum.

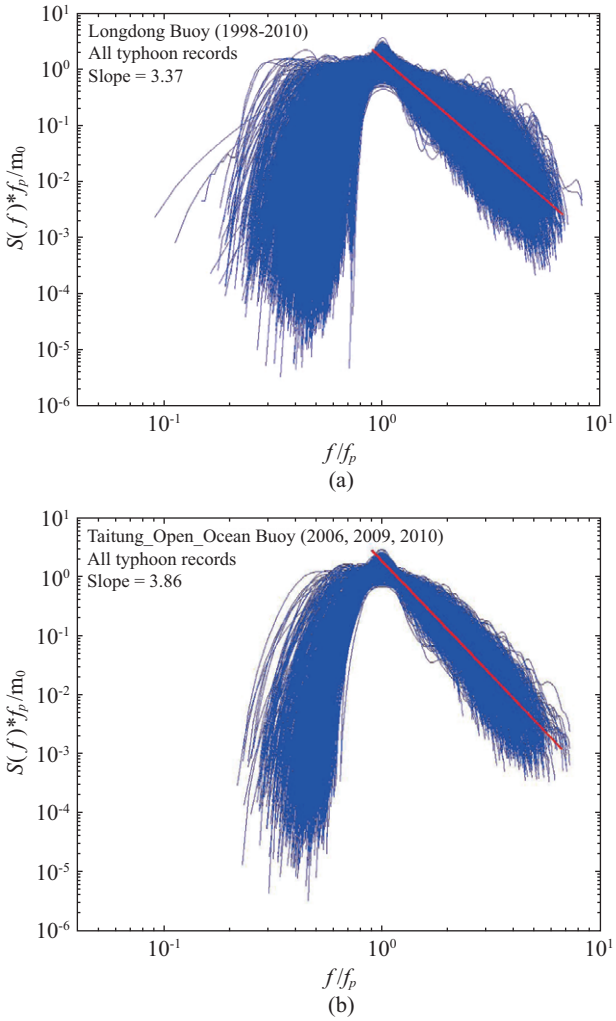

Fig. 11. Slope of the equilibrium range on the high-frequency side of the typhoon wave spectra (a) Longdong Buoy (Coastal buoy); (b) Taitung Deep Sea Buoy (Deep sea buoy).

The linear regression line was fitted to the normalized spectrum between the frequency range of $1.5f_p$ and $3f_p$. Fig. 11 shows the spectral slope for the high-frequency range at the Longdong and Taitung Deep Sea Buoys. The slope is -3.37 for the Longdong Buoy in shallow water and -3.86 for the Taitung Deep Sea Buoy in the open ocean. Table 3 shows the slopes for all buoys. It can be seen that wave spectra in relatively shallow water often exhibits an energy density decrease slower than f^{-4}, occasionally proportionally close to f^{-3} as in the Hsinchu Buoy (17 m) and the Longdong Buoy (23 m). This decrease is attributed to the effect of the water depth on the shape of the wave spectrum and to the interaction between the spectral components. Instead, the exponent is higher for the deep ocean buoys, such as -3.8 for the Xiaoliuqiu Buoy (-82 m), -3.84 for the Dongsha Buoy (-2600 m) and -3.86 for the Taitung Deep Sea Buoy (-5000 m).

Table. 3. Statistics of the energy spectral slope (f^{-n}).

Stations	Typhoon numbers	n
HL	82	3.72
HC	74	2.81
LD	77	3.37
GSD	55	3.08
DPB	52	3.50
XLC	39	3.80
MT	5	3.44
DS	5	3.84
ELB	84	3.70
TDS	12	3.86

2. Spectral Model

A parametric wave spectrum model is required for the wave prediction numerical models and laboratory experiments. Various spectral models such as the PM spectrum for fully developed sea, the JONSWAP for the fetch limited developing sea, as well as the Donelan spectrum, have been proposed. Because wave spectra observed in the field of fetch limited sea reveals a sharper peak than the PM spectrum, the JONSWAP spectrum model is examined to fit the field measurements. The JONSWAP spectral formulation is given as

$$S(f)=\alpha\frac{g^2}{(2\pi)^4}\frac{1}{f^5}\exp\left\{-1.25\left(\frac{f_p}{f}\right)^4\right\}\times\gamma^{\exp\left\{\frac{-(f-f_p)^2}{2(\sigma f_p)^2}\right\}} \quad (6)$$

where γ is the peak-enhancement factor, σ is the measure of the width of the peak, f_p is the spectral peak frequency, and α is a constant that relates to wind speed and fetch length.

Several methods (Acar, 1983; Moon and Oh, 1998; Violante-Carvalho et al., 2002; Feld and Mork, 2004) for fitting the observed spectra to a parametric model spectrum are based on the principle of minimizing the least square error between the measured and fitted spectra. The results of fitting are not significantly different between these methods. The method proposed by Moon and Oh (1998) is used by this study due to its smaller mean square error.

This study fits the JONSWAP spectrum model to the mean wave spectra at the time of highest sea state in each typhoon. Data are categorized into two groups: deep sea and shallow water. Data from the TDS, DS, and XLC buoys are grouped into the former, and the other buoys are in the shallow water group. Fig. 12 shows the individual and mean spectra for the deep sea buoys. The fitted JONSWAP spectrum is found to have the peak-enhancement factor $\gamma = 2.48$. For the shallow water buoys, $\gamma = 2.19$ fit the JONSWAP spectrum well. The γ values obtained for the typhoon waves in Taiwan are smaller than 3.3, which were obtained from the North Sea data. It is well known that when γ equals unity, the JONSWAP spectrum reduces to a fully developed PM spectrum. The results presented in this study suggests that the typhoon wave in Taiwan sea are in the developing stage. When a typhoon moves toward Taiwan, the wind speed always increases as the typhoon approaches the buoys. Although the wind is strong, the wind duration is not long enough for wave energy to become saturated.

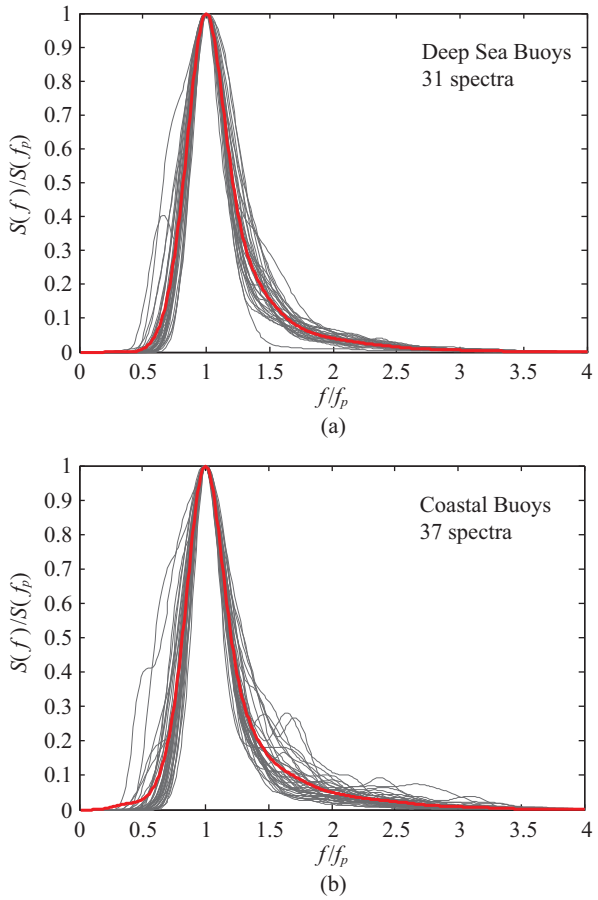

Fig. 12. The individual wave spectrua at the highest sea state during typhoons and their mean spectrua (red curve). (a) Deep sea buoys; (b) Coastal buoys.

VI. CONCLUSIONS

Typhoon generated waves, storm surge, and strong wind are the main natural impacts to coastal infrastructure and to ship navigation. Measurements of typhoon wave's parameters are necessary. This study analyzes typhoon generated waves observed by data buoys deployed in Taiwan sea. The longest record of the buoys is 18 years. More than 100 typhoon wave datasets were recorded.

The raw data from the buoys were re-analyzed to obtain higher resolution wave spectra in the frequency domain than those computed operationally on-board buoys. Quantitative comparisons show that the bias of significant wave height between the operational and re-analyzed results is 3.52% and 2.26% for the mean wave period. In addition, more than 70%

of the peak period biases are less than 0.01Hz and more than 70% of the dominant wave direction having biases less than 10 degrees. The statistical parameters from re-analysis do not significantly differ from those obtained on-board buoys, but they provide higher resolution spectra for future studies.

The study of the slope of the equilibrium range on the high-frequency side of a typhoon wave frequency spectrum was carried out in this research. The exponent n is less than 3.5 for those buoys located at the coastal waters; however, it is larger than 3.8 for the deep ocean buoys such as the Xiaoliuqiu Buoy (-82 m), the Dongsha Buoy (-2600 m) and the Taitung Deep Sea Buoy (-5000 m).

Typhoons do generate extreme waves. The maximum significant wave height observed during a typhoon was 23.94 m measured at the Gueisandao buoy station. However, a typhoon is a complex event that cannot be reduced to only a maximum wave height record. This study proposes two parameters to describe the severity of the typhoon sea state. They are the significant typhoon wave height (STWH) and the duration of large waves (DLW). Analysis on the parameters shows that the STWH are mainly between 2 to 4 m with the duration of 2 to 6 hours. Based on a scatter plot of the STWH versus the DLW, a limit curve for possible coastal area damage is found. With this curve before the arrival of a typhoon, it is possible to estimate the severity of the typhoon impact to the coast according to the proposed parameters that can be obtained from the wave forecasting model. Using these newly defined typhoon wave parameters, this study investigates the trend of typhoon sea state severity. The decadal variability on those typhoon wave parameters can be seen. However, much more observations are necessary to ascertain the decadal trend.

This study collects the frequency spectra of maximum wave heights during typhoons. The mean wave spectra are obtained for the deep sea and coastal ocean. The JONSWAP spectrum model is used to fit the field spectra to obtain a mathematical formula for use in oceanography and coastal engineering. The JONSWAP spectrum was found to fit well with the peak-enhancement factor $\gamma = 2.48$ for the deep sea and 2.19 for the coastal ocean. From the spectral parameters, it is known that the typhoon waves in the Taiwan sea are mainly in the developing stage.

ACKNOWLEDGMENTS

The authors would like to thank the Central Weather Bureau (MOTC-CWB-104-O-03) and the Ministry of Science and Technology (MOST 101-2628-E-006-024-MY3) for their support of this study.

REFERENCES

Acar, S. O. (1983). Statistical analysis of wind waves at Ordu and Akkuyu (Mersin). Master's thesis, Middle East Technical University, Turkey.

Allan, J. and P. D. Komar (2000). Are ocean wave heights increasing in the eastern North Pacific? Eos, Transactions American Geophysical Union 81, 561-567.

Babanin, A. V., T. W. Hsu, A. Roland, S. H. Ou, D. J. Doong and C. C. Kao (2011). Spectral wave modelling of typhoon Krosa. Natural Hazards and Earth System Science 11(2), 501-511.

Bacon, S. and D. J. T. Carter (1991). Wave climate changes in the North Atlantic and North Sea. Int. J. Climatol. 11, 545-558.

Carter, D. J. T. and L. Draper (1998). Has the North-East Atlantic become rougher? Nature 332, 494.

Doong, D. J., S. H. Chen, C. C. Kao and B. C. Lee (2007). Data quality check procedures of an operational coastal ocean monitoring network. Ocean Engineering 34, 234-246.

Feld, G. and G. Mørk (2004). A comparison of hindcast and measured wave spectra. 8th International Workshop on Wave Hindcasting and Forecasting, November 14-19, North Shore, Oahu, Hawaii, USA.

Grabemann, I. and R. Weisse (2008). Climate change impact on extreme wave conditions in the North Sea: an ensemble study. Ocean Dynamics 58, 199-212.

Holliday, N. P., M. J. Yelland, R. Pascal, V. R. Swail, P. K. Taylor, C. R. Griffiths and E. Kent (2006). Were extreme waves in the Rockall trough the largest ever recorded? Geophysical Research Letter 33.

Isobe, M., K. Kondo and K. Horikawa (1984). Extension of MLM for estimating directional wave spectrum, Proc. Symp. on Description and Modelling of Directional Seas, Copenhagen, A-6-1 - A-6-15.

Liu, P. C., H. C. Chen, D. J. Doong, C. C. Kao and G. Y. J. Hsu (2008). Monstrous ocean waves during typhoon Krosa. Ann. Geophys. 26, 1327-1329.

Longuet-Higgins, M. S., D. E. Cartwright and N. D. Smith (1963). Observations of the directional spectrum of sea waves using the motions of a floating buoy, Ocean Wave Spectra, Prentice-Hall, Englewood Cliffs, NJ.

Makin, V. K., V. N. Kudryavtsev and C. Mastenbroek (1995). Drag of the sea surface. Boundary-Layer Meteorology 73, 159-182.

Moon, I. J. and I. S. Oh (1998). A study of the characteristics of wave spectra over the seas around Korea by using a parametric spectrum method. Acta Oceanographica Taiwanica 37(1), 31-46.

Phillips, O. M. (1958). The equilibrium range in the spectrum of wind generated waves. Journal of Fluid Mechanics 4, 426-434.

Phillips, O. M. (1985). Spectral and statistical properties of the equilibrium range in the wind-generated gravity waves. Journal of Fluid Mechanics 156, 505-531.

Shemdin, O. H. (1977). Hurricane waves, storm surge and currents: An assessment of the state of the art. Proceedings of US-South East Asia Symposium on Engineering for Natural Hazards Protection, Manilia.

Toba, Y. (1973). Local balance in the air-sea boundary processes, III, On the spectrum of wind waves. Journal of the Oceanographic Society of Japan 29, 209-225.

Violante-Carvalho, N., F. J. Ocampo-Torres and I. S. Robinson (2004). Buoy observations of the influence of swell on wind waves in the open ocean. Applied Ocean Research 26, 49-60.

Wang, D. W., D. A. Mitchell, W. J. Teague, E. Jarosz and M. S. Hulbert (2005). Extreme waves under Hurricane Ivan. Science 309, 896.

Wang, X. and V. Swail (2006). Climate change signal and uncertainty in projections of ocean wave heights. Climate Dynamic 26, 109-126.

Ward, E. G. (1974). Ocean data gathering program – an overview. Proceedings of 6th Offshore Technology Conference, Houston, TX.

Weisse, R. and H. Günther (2007). Wave climate and long-term changes for the Southern North Sea obtained from high resolution hindcast 1958-2002. Ocean Dynamic 57, 161-172.

Weisse, R., H. von Storch and F. Feser (2005). Northeast Atlantic and North Sea storminess as simulated by a regional climate model 1958-2001 and comparison with observations. Journal of Climate 18, 465-479.

Young, I. R. (1998). Observations of the spectra of hurricane generated waves. Ocean Engineering 25, 261-276.

Young, I. R. (2003). A review of the sea state generated by hurricanes. Marine Structures 16, 201-218.